14th International Symposium on Turbulence and Shear Flow Phenomena (TSFP14)
Heidelberg, Germany, July 28–31, 2026

# EXTENDING THE DYNAMICAL SYSTEMS VIEW OF TURBULENCE TO LARGE DOMAINS

**Dmitriy Zhigunov**
School of Mathematics
University of Edinburgh
Edinburgh
EH9 3FD, UK
dmitriy.zhigunov@ed.ac.uk

**Rich Kerswell**
DAMTP
University of Cambridge
Cambridge
CB3 0WA, UK
r.r.kerswell@damtp.cam.ac.uk

**Jacob Page**
School of Mathematics
University of Edinburgh
Edinburgh
EH9 3FD, UK
jacob.page@ed.ac.uk

## ABSTRACT

The combination of gradient-based optimisation with differentiable flow solvers has dramatically expanded the number of known simple invariant solutions in two-dimensional Kolmogorov flow, with hundreds of relative periodic orbits (RPOs) now converged (Page *et al.*, 2024*b*). These solutions – all found on the canonical $2\pi \times 2\pi$ domain – provide robust statistical reconstructions of the flow at the Reynolds numbers (*Re*) where they were converged. It is generally accepted that the application of these ideas to spatially-extended systems will require a superposition of smaller-scale structures in *space* as well as time. In this spirit, we explore the degree to which Kolmogorov flow in large boxes can be described locally by small-box dynamics, performing direct numerical simulations of two-dimensional turbulence in boxes of size $8\pi \times 8\pi$ and $16\pi \times 16\pi$ at $Re = 40$. These flows spend extended periods in a high dissipation 'bursting' state, in which the flow qualitatively resembles the small box simulations on small $2\pi \times 2\pi$ patches. We show that this observation holds quantitatively using conditional vortex statistics, conditioning on whether the flow is locally (in space) bursting or not. We then seek to make a stronger connection to the small box dynamics using our extensive library of RPOs. First, we show that large numbers of small box, high-dissipation solutions can be vertically 'glued' together to build either new simple invariant sets. We construct many new $2\pi \times 4\pi$ RPOs from a small-box RPO and the laminar solution, before adding additional laminar tiles incrementally in the vertical. These solutions appear to be robust to this process, i.e. they can embedded in arbitrarily tall vertical domains. We then identify a set of new-candidates for small-box traveling waves using a combination of local recurrence analysis and an autoencoder to generate plausible small-box initial conditions. Our results are a first step in building a space-time tapestry of Kolmogorov turbulence from a collection of small-box exact coherent states.

## BACKGROUND

The dynamical systems view of turbulence is an approach that promises to connect the dynamics of coherent structures to statistical properties of the flow. One imagines the turbulence as a 'pinball' in a very high-dimensional state space, bouncing between states which are exact, unstable solutions of the Navier-Stokes equations (see Kawahara *et al.*, 2012; Graham & Floryan, 2021, for an overview of the field). Each exact solution isolates a particular recurrent process in the flow.

A long-standing challenge has been the identification and convergence of the exact unstable solutions that underpin these ideas, with early algorithms being ineffective at higher *Re*. Recently many more solutions were found in a turbulent two-dimensional Kolmogorov flow using a combination of (i) gradient-based optimization and a fully differentiable flow solver (Page *et al.*, 2024*b*) and (ii) use of convolutional neural networks to detect near recurrences (Page *et al.*, 2024*a*). This large collection of solutions can be used to accurately predict full probability density functions for the flow, lending real weight to the pinball view of turbulence, at least for small domains.

While much of the literature has focused on exact solutions in so-called 'minimal' boxes, both in 2D (Chandler & Kerswell, 2013; Lucas & Kerswell, 2015) and 3D (Kawahara & Kida, 2001; Park & Graham, 2015), there have been recent attempts to extend the search for exact solutions to larger domains. The majority of these solutions have been found by careful manipulation and continuation of minimal box states (e.g. Schneider *et al.*, 2010; Avila *et al.*, 2013). As a result, they are dominated by a single cross-shear lengthscale. The multiple interacting 'substructures' observed in turbulence in spatially extended domains are absent.

In this work we perform large-box simulations of Kolmogorov flow in an effort to assess the relevance of the small box dynamics, and its extensive collection of exact solutions, in larger domains. The large-domain is an interesting dynamical system in itself, with the flow spending extended periods in a quiescent state before bursting into domain-filling chaos featuring large numbers of small-scale vortices. In these high-dissipation events, the flow locally resembles the dynamics in the small box, which we demonstrate quantitatively here via a statistical analysis of vortices in the flow, conditioning on the local dissipation.

We then attempt to 'realise' small box exact solutions in the larger domain. We do this in two ways: First, we show how high-dissipation RPOs from the small box can be tiled vertically – apparently indefinitely – with patches of the laminar flow. Second, we search directly for near recurrences in moving boxes in the larger domains. We generate large numbers of candidates for small box traveling waves in this way. These ideas build on the promising space-time tiling of the Kuramoto-Sivashinsky equation performed by Gudorf & Cvitanovic (2019).

## SETUP

The flow configuration considered in this work is two-dimensional Kolmogorov flow. This flow is driven by a monochromatic body force in the horizontal ($x$) direction. The out-of-plane vorticity equation is

$$\partial_t \omega + \mathbf{u} \cdot \nabla \omega = \frac{1}{Re} \Delta \omega - n \cos(ny) \qquad (1)$$

The velocity $\mathbf{u} = (u, v)$ is obtained from the vorticity via solution of the Poisson equation $\mathbf{u} = -\nabla \times (\Delta^{-1} \omega \hat{\mathbf{z}})$. The number of forcing waves is $n = 4$ and the problem has been non-dimensionalised by the fundamental wavenumber associated with height of the (unit aspect ratio) reference box, $k^*$, and the (dimensional) strength of the forcing, $\chi^*$, resulting in a definition of $Re := \sqrt{\chi^*/k^{*3}}/\nu$, where $\nu$ is the kinematic viscosity.

We consider 'small-box' Kolmogorov flow in a box of $2\pi \times 2\pi$ (the 'reference' box) where large numbers of exact unstable solutions, primarily periodic orbits, have been converged (Page *et al.*, 2024*b*). We also consider larger, equal aspect ratio boxes of width $8\pi$ and $16\pi$, where we continue to the use reference scales for the small box in the non-dimensionalization. Most of the statistical analysis is performed in the smaller ($8\pi$) of the two large domains: we will see that the high dissipation events in that geometry can locally appear to be very similar regardless of box size.

We use the Dedalus PDE solver for all of our calculations (Burns *et al.*, 2020). Due to the periodicity in $x$ and $y$, Fourier decompositions are employed in both directions with $N_x = N_y = 128$ gridpoints per $2\pi$ box. A third-order, operator-splitting Runge Kutta scheme is used for time advancement.

## LARGE BOX SIMULATIONS

We first examine global properties of the flow in larger domains: A time series of dissipation, $D := (A\,Re)^{-1} \iint |\nabla \mathbf{u}|^2 d^2\mathbf{x}$ ($A$ is domain area), normalized by its value in laminar flow, $D_l$, is reported in figure 1 for both the minimal $2\pi \times 2\pi$ box and the larger box of width $8\pi$. In both cases, the flow spends extended periods of time in a low-dissipation state, interspersed with high-dissipation 'bursts'.

Snapshots of the out-of-plane vorticity before and during a bursting event in both geometries are also shown in figure 1. In the large domain, the quiescent dynamics (panel ①) are reminiscent of the low-dissipation dynamics in small-box Kolmogorov flow shown directly above (see also Chandler & Kerswell, 2013; Page *et al.*, 2021): the vorticity is organized in a pair of opposite-signed slanted patterns, with some large-scale organization into a pair of vortices. The signature of the monochromatic forcing function is clearly apparent. In this regime the dynamics in the larger box are clearly distinct from the small-box simulations: the flow feels the effects of the global geometry.

Panels ② – ④ in figure 1 show the vorticity entering/during/leaving a high-dissipation event. In the larger box, the 'burst' in global dissipation is associated with the formation of additional small-scale vorticies on large-scale slanted structures (②), which then rapidly contaminate the rest of the flow. During the high-dissipation regime these small scale structures are interspersed with smaller quiescent patches (③). The small scale structures eventually decay and the quiescent regions expand as the flow relaxes back to the calmer low-dissipation dynamics (④).

This qualitative picture appears to extend to even larger boxes – an example snapshot in a large $16\pi$-width box is reported in figure 2. Again, in a high-dissipation event the flow consists of extended quiescent patches interspersed with high dissipation regions containing many interacting smaller vortices.

What is striking about the high-dissipation events in these large-scale Kolmogorov flows is how qualitatively similar they are to high-dissipation events in the canonical $2\pi \times 2\pi$ box – see the panels directly above for a high-dissipation, small box event (and also Chandler & Kerswell, 2013; Page *et al.*, 2021; Cleary & Page, 2025). To probe this apparent similarity further, we reconstruct $2\pi \times 2\pi$ patches of the large $16\pi$-width box snapshots using an autoencoder trained on small-box data only. This model was originally introduced in Page *et al.* (2024*a*). It is an approximation to the identity function in the small domain, $\mathscr{A}(\omega_{\text{small box}}) \approx \omega_{\text{small box}}$, with forced dimensionality reduction down to 128 degrees of freedom, and results in relative reconstruction errors of $O(2\%)$ in the small box.

The output of this model applied to patches of the large box snapshot is also shown in figure 2. There are some boundary artifacts (the model enforces periodicity in its output) but the reconstruction is good – relative errors are similar to the small box – despite the model being trained only on small box data.

Our objective is to assess to what degree these qualitative observations hold quantitatively. We attempt to do this in two ways: (1) using conditional statistics to show the similarity in high dissipation patches of the flow to bursts in the small box and (2) by attempting to show that the large flow bursts can be understood in terms of *exact unstable solutions* from the small box.

## CONDITIONAL STATISTICS

Our observations above imply that similarity between the small- and large-box computations applies only in particular spatial regions of the large domain. We therefore compute conditional statistics based on local values of the dissipation rate, splitting snapshots of the $8\pi \times 8\pi$ flow domain into $4 \times 4$ small-box tiles $\{\Omega_i\}_{i=1}^{16}$ (each of size $2\pi \times 2\pi$). We then label the flow locally as 'high-dissipation' if $D_{\Omega_i} := \iint_{\Omega_i} |\omega|^2 d^2\mathbf{x} \geq 0.15 D_{\Omega_i,l}$. This is the same bursting classifier we have used in previous work (Page *et al.*, 2021, 2024*b*). An example domain-decomposition into 'high' and 'low' dissipation regions is reported in figure 3.

Conditioning on the local dissipation allows us to demonstrate that the vortices, which dominate the flow in high-

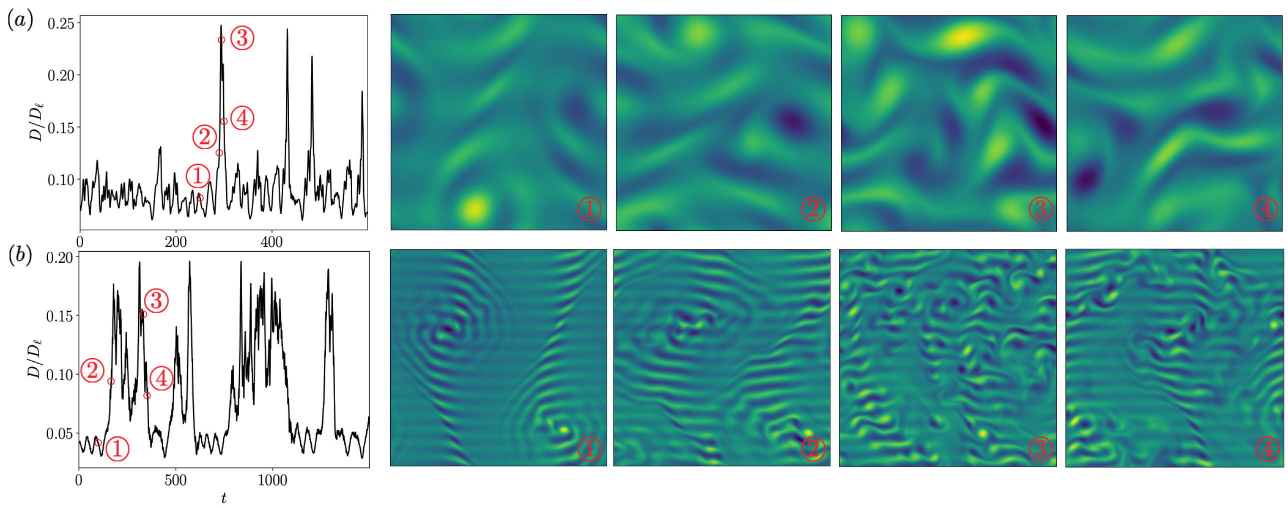


Figure 1. (Left) Time series of global dissipation, normalized by the value in a laminar flow, $D_l$. (Right) Out-of-plane vorticity at the four times identified with red symbols in the left panel. Contours runs $11.4 \leq \omega \leq 11.4$ (a) Shows time evolution in the small $2\pi \times 2\pi$ box, (b) the evolution in the larger $8\pi \times 8\pi$ domain.

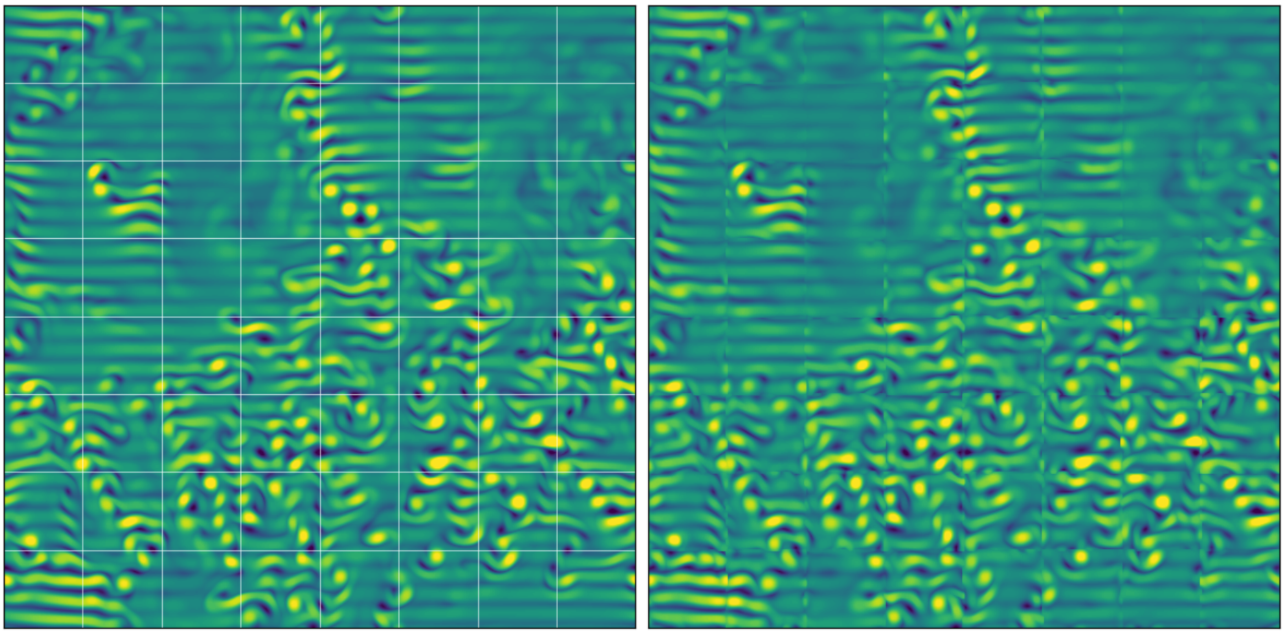

Figure 2. (Left) Out-of-plane vorticity in large-box ($16\pi \times 16\pi$) Kolmogorov flow. Thin white lines highlight the reference 'small box' ($2\pi \times 2\pi$) scale. (Right) Reconstruction of the snapshot at left by passing each masked $2\pi \times 2\pi$ region through an autoencoder, $\mathscr{A}(\mathscr{M}\omega)$. The output of the autoencoder is periodic in both $x$ and $y$, which results in small discontinuities between masked regions.

dissipation bursts, are statistically similar in the small and larger ($8\pi$-wide) boxes. To extract the vortices, we follow the approach of Page *et al.* (2024*a*) and identify 'vortices' as connected regions of the flow where $\omega - \overline{\omega} > 2\omega_{RMS}$ (here $\overline{\omega}$ is a time-and-symmetry averaged field).

In figure 4 we report the (unconditioned) statistical properties of vortices in both the full domain in the small and large (width $8\pi$) boxes, showing estimated probability density functions (PDFs) for their areas and circulations. Unsurprisingly, there are some notable differences between the geometries: perhaps most striking is the difference in area, with (i) vortices in the larger domain tending to be larger – the distant periodic boundaries do not restrict the structures as they do for the smaller box – and (ii) small vortices appearing below the cutoff $\omega_{RMS}$ in the larger box.

A better demonstration of the statistical similarity of the vortices in the large domain to the small box emerges under conditional averaging. For regions which are locally bursting either in the small-box or in patches of the larger box, both PDFs are similar in structure, with similar means, modal contributions and tails. This observation is in line with visual observations within the snapshots (figures 1 and 2) and partially explains why the autoencoder is able to reconstruct patches of the larger boxes so faithfully.

## EXACT SOLUTIONS IN TALL BOXES

One of the central goals of this work is to assess to what degree small-box *exact unstable solutions* are relevant in larger computations. The conditional statistics described above give us reason to be optimistic here, at least for the high dissipation events, though we are also motivated by the 'space-time tiling'

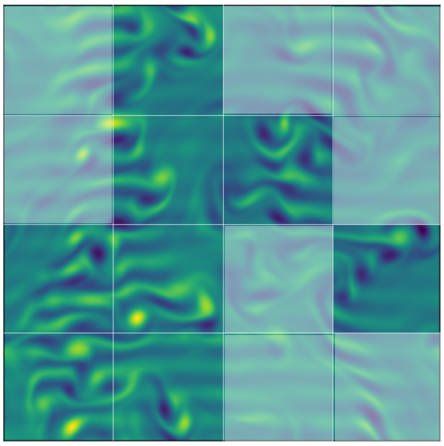

Figure 3. Example out-of-plane vorticity snapshot showing domain masking for conditional statistics. Non-faded regions identity local ‘high dissipation’ patches in an $8\pi \times 8\pi$ computation.

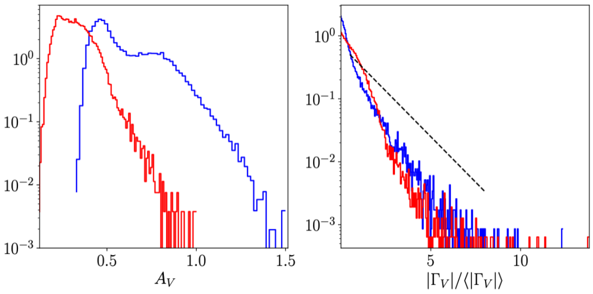


Figure 4. Statistics of ‘vortices’ in the $2\pi \times 2\pi$ box (red) and the $8\pi \times 8\pi$ box (blue). See text for description of how vortices are extracted. Shown are PDFs of the vortex areas, $A_V$, and absolute value of the vortex circulations, $|\Gamma_V|$. The dashed line in the circulation PDFs is $\exp\left(-(2/3)|\Gamma_V|/\langle|\Gamma_V|\rangle\right)$, a scaling observed in decaying turbulence by Jiménez (2020).

of turbulence by exact solutions advocated in e.g. Gudorf & Cvitanovic (2019).

In the minimal $2\pi$ box, large numbers of unstable solutions have been used to reconstruct the statistics of the chaotic attractor. This was done in Page *et al.* (2024*b*) by labeling a turbulent trajectory by the ‘nearest’ unstable solution (here *relative* periodic orbits) to create a Markov chain model of the flow. In this model the states are the exact solutions, with weights for statistical reconstructions set by the invariant measure of the chain.

Relative periodic orbits (RPO) are solutions of (1) for which $\mathscr{T}^{\alpha}\varphi_T(\omega) - \omega = 0$, where $\varphi_t$ is the time-forward map associated with (1), $T$ the period of the RPO and $\alpha$ the horizontal shift ($\mathscr{T}^{\alpha}: \omega(x,y) \to \omega(x+\alpha, y)$). The library of solutions used in this work was originally reported in Page *et al.* (2024*b*) and Page *et al.* (2024*a*), and features 174 RPOs at $Re = 40$. The majority of solutions were found by minimization of a scalar loss function of the form

$$\mathscr{L}(\omega, T, \alpha) := \frac{\|\mathscr{T}^{\alpha}\varphi_T(\omega) - \omega\|}{\|\omega\|}, \tag{2}$$

using a high-dimensional Newton-Raphson algorithm to solve for exact roots $(\omega, T, \alpha)$ of $\mathscr{T}^{\alpha}\varphi_T(\omega) - \omega = 0$. This initial minimization of( (2) was done by gradient optimisation through a fully differentiable flow solver (JAX-CFD, see Kochkov *et al.*, 2021).

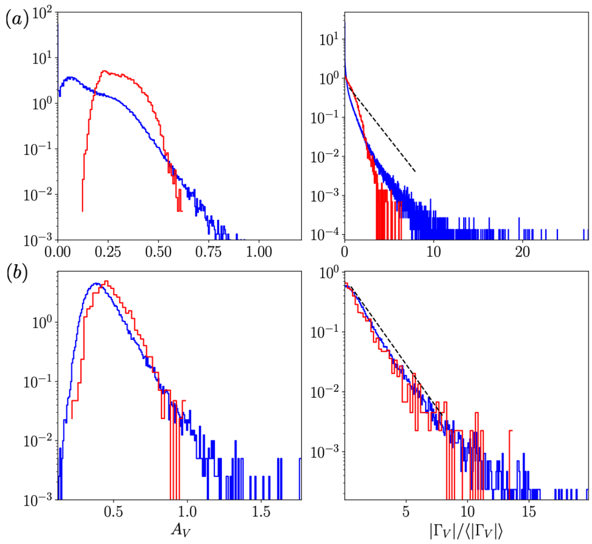


Figure 5. Conditional statistics of ‘vortices’ in the $2\pi \times 2\pi$ box (red) and the $8\pi \times 8\pi$ box (blue). See text for description of how vortices are extracted. Shown are PDFs of the vortex areas, $A_V$, and absolute value of the vortex circulations, $|\Gamma_V|$. Statistics are conditioned on $D/D_l \leq 0.15$ (a) and $D/D_l > 0.15$ (b). The $8\pi \times 8\pi$ domain is first partitioned into $4 \times 4$ $2\pi \times 2\pi$ patches, and the conditioning is done locally per-patch. The dashed line in the circulation PDFs is $\exp\left(-(2/3)|\Gamma_V|/\langle|\Gamma_V|\rangle\right)$, the scaling observed in decaying turbulence by Jiménez (2020).

We attempt to extend solutions from this small-box library in the vertical. This is different from parameter continuation (e.g. done via continuous variation of *Re*, or domain width), because it involves the addition of new discrete ‘bands’ of forcing. The computational method used is again a combination of optimisation and a Newton algorithm, and is outlined carefully in Zhigunov & Page (2026).

We show in figure 6 five exact RPOs in a box of height $4\pi$, which result from combining a small-box RPO and a laminar patch. All starting RPOs are high dissipation, $D/D_l$, and the successful tiling of these states with the laminar solution was attributed by Zhigunov & Page (2026) to the relatively weak induced velocity associated with the large number of small-scale vortices creating a shielding effect. Note the similarity between these states and the high dissipation patches observed in the large computations (figures 1 and 2) – the vortices have a length scale set by the forcing, not the domain size.

We go further here and add additional laminar stripes incrementally. While the original attachment of the laminar tile reported in figure 6 required quite careful treatment to ensure convergence (optimisation followed by the Newton algorithm), the addition of further laminar bars gets easier incrementally (we add bars at the point farthest from the embedded RPO). Convergence is complete in a few Newton steps.

We show in figure 7 the result of this procedure, where we have successfully extended the vertical domain of a pair of small-box RPOs to a domain height of $8\pi$. The procedure has worked for every high-dissipation state from Zhigunov & Page (2026) we have tried so far. We believe that the procedure can be continued indefinitely; convergence is easier with each

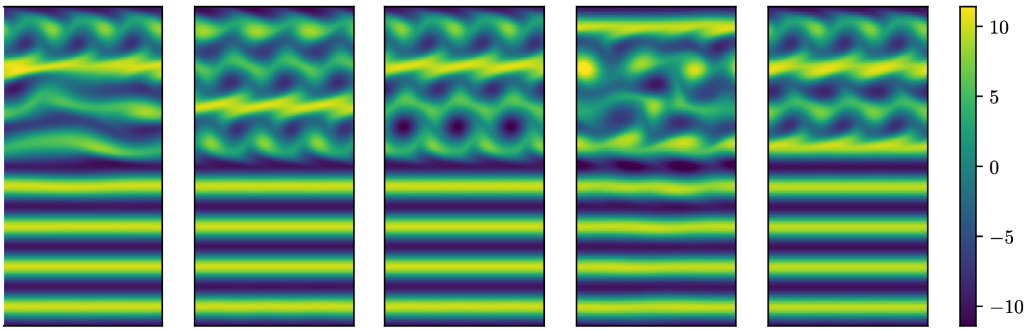


Figure 6. Snapshots from five exact RPOs on a $2\pi \times 4\pi$ domain resulting from the spatial tiling of a high-dissipation $2\pi \times 2\pi$ RPO with the laminar state. Out-of-plane vorticity is shown in all cases.

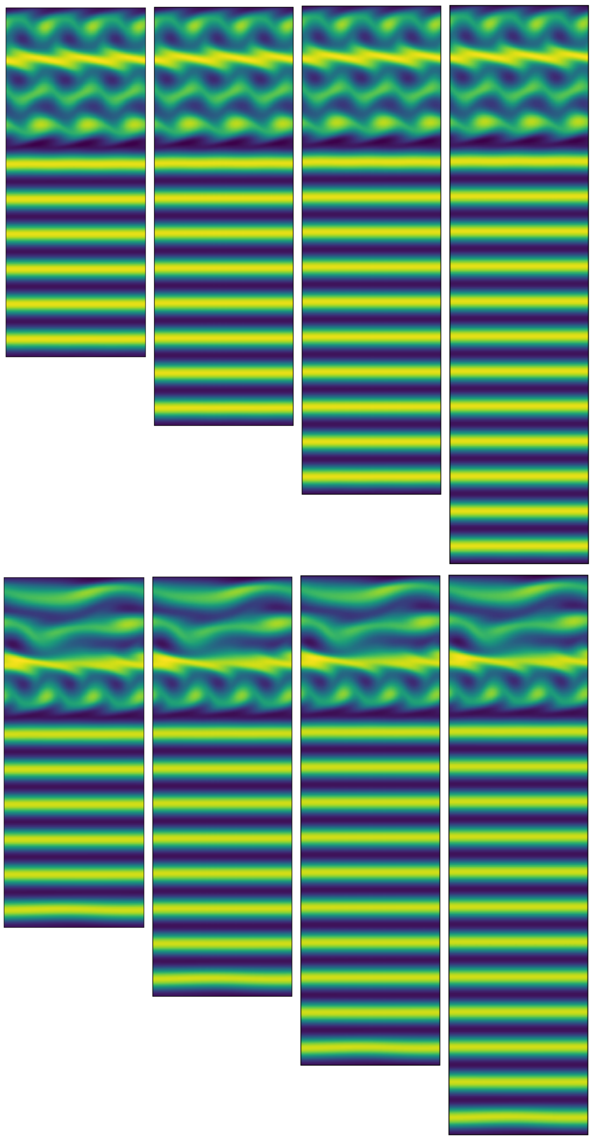

Figure 7. Two examples of RPOs which can be tiled repeatedly with laminar flow. Convergence in an $8\pi$ domain (rightmost panels) is achieved incrementally by adding single $\pi/2$-high stripes of the laminar profile. We show intermediate states at $5\pi$, $6\pi$ and $7\pi$ (from left). The final solutions in the tallest box have periods $T = 1.96$ (top) and $T = 2.70$ (bottom) with horizontal shifts of $\alpha = 1.52$ and $\alpha = -0.56$ respectively.

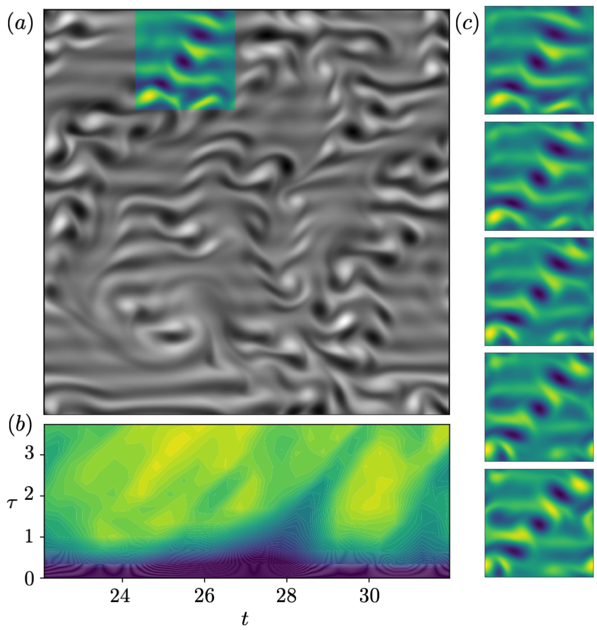


Figure 8. Small-box exact solution candidate identified in the large box. (a) Out-of-plane vorticity in the $8\pi \times 8\pi$ domain, with the colored $2\pi \times 2\pi$ region identifying a candidate small-scale traveling wave. (b) Contours of autorecurrence in a shifting box, $R(t,\tau) = \|\mathscr{M}(\omega(t) - \omega(t-\tau))\| / \|\mathscr{M}\omega(t)\|$ . Contour levels run from 0.1 to 0.32. (c) Snapshots of the candidate structure at $t = 26.18 + 0.34n$ ($n \in \{0,\ldots,4\}$) in a $2\pi \times 2\pi$ box, created by applying the autoencoder to the masked region in (a).

successive laminar stripe.

The approach should be contrasted with localised exact coherent states which have been obtained in canonical shear flows (e.g. Schneider *et al.*, 2010; Avila *et al.*, 2013). In those cases, guesses for localised states are obtained by windowing known exact solutions. Here, we are adding non-trivial flow structure incrementally, rather than a straightforward parameter continuation. We are currently exploring a combination of *both* approaches in order to demonstrate dual localisation in both directions of the high-dissipation states.

## CANDIDATE SMALL-BOX SOLUTIONS FROM LARGE BOXES

Finally, we outline a procedure for identifying candidate small-box solutions from the large domain computations. We do this by looking for near recurrences in masked patches, $\mathscr{M}\omega$, of the larger $8\pi \times 8\pi$ domain. We search over the discrete symmetries in the flow and sweep our mask horizontally to account for propagation of structure through the domain. An example of this procedure is reported in figure 8, where a candidate small-scale traveling wave is identified (the autorecurrence, $R(t,\tau) \leq 0.15$ over $\sim 3$ advective time units. To convert this into a viable initial condition for the small-box computations we apply the autoencoder described earlier, $\omega^0_{\text{small box}} = \mathscr{A}(\mathscr{M}(\omega))$, which enforces periodic boundary conditions while preserving the spatial structure. We have generated many promising candidates for exact small-box solutions in this way and will report on their convergence rates at the meeting,

## CONCLUSIONS

In this paper we have examined Kolmogorov flow in spatially extended domains. The large-box system repeatedly exhibits high-dissipation bursts away from a domain-filling coherent state. These high dissipation bursts were shown to be similar in character locally – in terms of their vortex statistics – to high dissipation events in a much smaller 'minimal' Kolmogorov flow in the canonical $2\pi \times 2\pi$ box.

Motivated by the apparent similarity of small patches of the large scale flow to the smaller computations, we sought to apply ideas from dyanmical systems theory to the extended domains. We did this in two ways, first by showing how many small box RPOs can be stacked with the laminar solution on increasingly tall domains. This process is surprisingly robust and can be performed for a large number of small box states. We also proposed a method using a combination of masked autorecurrence and an autoencoder (trained on small box data) to generate candidate guesses for exact coherent states in the small box directly from large-scale computations.

These ideas set the stage for an examination of spatially extended flows using the techniques from dynamical systems. We hope the computational methods outlined here can help realize the space-time tapestry view of turbulence – in which exact solutions tile spacetime – outlined in recent work (Liang & Cvitanović, 2022).

## REFERENCES

Avila, M., Mellibovsky, F., Roland, N. & Hof, B. 2013 Streamwise-Localized Solutions at the Onset of Turbulence in Pipe Flow. *Phys. Rev. Lett.* **110**, 224502.

Burns, Keaton J., Vasil, Geoffrey M., Oishi, Jeffrey S., Lecoanet, Daniel & Brown, Benjamin P. 2020 Dedalus: A flexible framework for numerical simulations with spectral methods. *Physical Review Research* **2** (2).

Chandler, G. J. & Kerswell, R. R. 2013 Invariant recurrent solutions embedded in a turbulent two-dimensional Kolmogorov flow. *Journal of Fluid Mechanics* **722**, 554–595.

Cleary, Andrew & Page, Jacob 2025 Dynamical relevance of periodic orbits under increasing reynolds number and connections to inviscid dynamics. *Journal of Fluid Mechanics* **1020**.

Graham, Michael D. & Floryan, Daniel 2021 Exact coherent states and the nonlinear dynamics of wall-bounded turbulent flows. *Annual Review of Fluid Mechanics* **53** (1), 227–253.

Gudorf, Matthew & Cvitanovic, Predrag 2019 Spatiotemporal tiling of the Kuramoto-Sivashinsky equation. In *APS March Meeting Abstracts*, *APS Meeting Abstracts*, vol. 2019, p. L70.263.

Jiménez, Javier 2020 Dipoles and streams in two-dimensional turbulence. *Journal of Fluid Mechanics* **904**, A39.

Kawahara, G. & Kida, S. 2001 Periodic motion embedded in plane Couette turbulence: regeneration cycle and burst. *Journal of Fluid Mechanics* **449**, 291–300.

Kawahara, G., Uhlmann, M. & van Veen, L. 2012 The significance of simple invariant solutions in turbulent flows. *Annual Review of Fluid Mechanics* **44** (1), 203–225.

Kochkov, Dmitrii, Smith, Jamie A., Alieva, Ayya, Wang, Qing, Brenner, Michael P. & Hoyer, Stephan 2021 Machine learning–accelerated computational fluid dynamics. *Proceedings of the National Academy of Sciences* **118** (21).

Liang, H & Cvitanović, P 2022 A chaotic lattice field theory in one dimension. *Journal of Physics A: Mathematical and Theoretical* **55** (30), 304002.

Lucas, Dan & Kerswell, Rich R. 2015 Recurrent flow analysis in spatiotemporally chaotic 2-dimensional kolmogorov flow. *Physics of Fluids* **27** (4), 045106.

Page, J., Brenner, M. P. & Kerswell, R. R. 2021 Revealing the state space of turbulence using machine learning. *Physical Review Fluids* **6**, 034402.

Page, Jacob, Holey, Joe, Brenner, Michael P. & Kerswell, Rich R. 2024*a* Exact coherent structures in two-dimensional turbulence identified with convolutional autoencoders. *Journal of Fluid Mechanics* **991**, A10.

Page, Jacob, Norgaard, Peter, Brenner, Michael P. & Kerswell, Rich R. 2024*b* Recurrent flow patterns as a basis for two-dimensional turbulence: Predicting statistics from structures. *Proceedings of the National Academy of Sciences* **121** (23), e2320007121.

Park, Jae Sung & Graham, Michael D. 2015 Exact coherent states and connections to turbulent dynamics in minimal channel flow. *Journal of Fluid Mechanics* **782**, 430–454.

Schneider, Tobias M., Gibson, John F. & Burke, John 2010 Snakes and ladders: Localized solutions of plane couette flow. *Phys. Rev. Lett.* **104**, 104501.

Zhigunov, Dmitriy & Page, Jacob 2026 Exact coherent structures as building blocks of turbulence on large domains. *arXiv preprint* .